

L_X - T Relation and Thermal Evolution of Galaxy Clusters

Naomi Ota^{1,2}*, Tetsu Kitayama³, Kuniaki Masai⁴ and Kazuhisa Mitsuda¹

¹ ISAS/JAXA, 3-1-1 Yoshinodai, Sagamihara, Kanagawa 229-8510, Japan

² MPE, Postfach 1312, 85748 Garching, Germany (Present address)

³ Toho University, 2-2-1 Miyama, Funabashi, Chiba 274-8510, Japan

⁴ Tokyo Metropolitan University, 1-1 Minami-osawa, Hachioji, Tokyo 192-0397, Japan

Abstract We present an observational approach to constrain the global structure and evolution of the intracluster medium utilizing the *ROSAT* and *ASCA* distant cluster sample. From statistical analysis of the gas density profile and the connection to the L_X - T relation under the β -model, the scaled gas profile is found to be nearly universal for the outer region. On the other hand, a large density scatter exists in the core region and there is clearly a deviation from the self-similar scaling for clusters with a small core. The discovery of the existence of an X-ray fundamental plane in the distant cluster sample suggests that the cooling time (t_{cool}) is a parameter to control the gas structure. The appearance of small cores in regular clusters may be strongly connected with the thermal evolution. We derive the luminosity-ambient temperature (T') relation, assuming the universal temperature profile for the clusters with short t_{cool} , and find the dispersion around the relation significantly decreases and the slope becomes marginally less steep. Considering a correlation between t_{cool} and the X-ray morphology, the observational results lead us to draw a phenomenological picture: after a cluster collapses and t_{cool} falls below the age of the universe, the core cools radiatively with quasi-hydrostatic balancing in the gravitational potential, and the central density gradually becomes higher to evolve from an outer-core-dominant cluster, which follows the self-similarity, to inner-core-dominant cluster.

Key words: galaxies: clusters: general — X-rays: galaxies: clusters

1 INTRODUCTION

Clusters of galaxies are the largest gravitationally bound systems in the Universe. This makes them very important probes of cosmology. Thus a precise knowledge of their masses is very important to measure the large-scale structure and to test cosmological models (see Voit 2005 for review). In linking the cluster mass with observables, X-ray observations play an indispensable role since the clusters are in general strong X-ray sources and their luminosity and temperature, which are expected to be mass proxies, can be measured for a larger number of clusters. However, there are increasing pieces of evidences that evolution of the X-ray emitting gas is fairly complex due to radiative cooling effect, merger activity and so on. Therefore it is necessary to examine such non-gravitational effects in scaling relations of galaxy clusters.

The L_X - T relation of clusters of galaxies is one of the most fundamental parameter correlations established from previous X-ray observations (e.g., Edge et al. 1990). Since the X-ray luminosity reflects temperature and density profiles of hot intracluster medium (ICM), the L_X - T relation should contain information on the physical status and evolution of the ICM. Observationally, the correlation is well approximated with a power-law function: $L_X \propto T^\alpha$ with $\alpha \sim 3$ and shows a significant scatter around the mean relation. On the other hand, the self-similar model predicts $\alpha = 2$ (Kaiser 1986). Thus the inconsistency between

* E-mail: ota@astro.isas.jaxa.jp

the observations and the simple theoretical model has been debated for many years and many ideas have been proposed, including non-gravitational heating, dependence of gas mass fraction on the temperature, and the effect of radiative cooling (e.g., Evrard & Henry 1991; Cavaliere et al. 1997; David et al. 1993; Neumann & Arnaud 2001). To understand the origin of the observed scatter, we consider that the following two observational facts will give a important clue: one is the connection between the cluster core size and the normalization factor of the L_X-T relation as pointed out by Ota & Mitsuda (2002; see also Fig. 1a) and the other is a drop in temperature by a factor of ~ 3 at the center of many relaxed clusters found from high-sensitivity *XMM-Newton* and *Chandra* observations (‘universal temperature profile’; e.g., Kaastra et al. 2004). These results indicate that the gas evolution in the core region have a great impact on the L_X-T relation particularly under the radiative cooling. Aiming at further constraining the gas structure and the thermal evolution, we performed a detailed statistical analysis based on the large distant cluster sample.

We use $\Omega_M = 0.3$, $\Omega_\Lambda = 0.7$ and $h_{70} \equiv H_0/(70 \text{ km s}^{-1} \text{ Mpc}^{-1}) = 1$. The quoted parameter errors are the 90% confidence range throughout the paper unless otherwise noted. The 1σ error bars are plotted in all figures.

2 THE DISTANT CLUSTER SAMPLE AND THE REDSHIFT DEPENDENCE

The sample is selected from an X-ray catalog of the *ROSAT* and *ASCA* distant clusters presented in Ota & Mitsuda (2004). Although the original catalog includes 79 clusters in the redshift range of $0.1 < z < 0.82$, the final sample used in this work comprises 69 clusters in $0.1 < z < 0.56$ in order to reduce possible selection effect and measurement uncertainties that are more serious at higher redshifts.

The data analysis consists of two major steps: (1) the spatial analysis with the *ROSAT* HRI and (2) the spectral analysis with the *ASCA* GIS and SIS detectors. For (1), the radially-averaged X-ray surface brightness distribution was fitted with the isothermal β -model (Cavaliere & Fusco-Femiano 1976) to determine the slope parameter β , the core radius r_c and the central surface brightness. The model gives a reasonably good fit to the observed surface brightness of many clusters: it results in a statistically acceptable fit for about 2/3 of the sample. For some clusters, however, it has left residual emission in the central region and a significant improvement was found when including an additional β -model component particularly for 9 clusters (termed as ‘‘double- β ’’ clusters). The present work basically stands on the single β -model for the reason that we are mainly interested in a systematic study on the global structure in a large number of distant clusters. Furthermore, the X-ray morphology was measured with using ‘centroid variations’ of the cluster image and the sample was classified into ‘‘regular’’ and ‘‘irregular’’ clusters.

For (2), the emission-weighted temperature and bolometric luminosity were measured from the *ASCA* spectroscopic data under the Raymond-Smith model. kT is the emission-weighted temperature determined from the simultaneous fitting to the *ASCA* GIS and SIS spectra extracted from $r < 6'$ and $r < 3'$ circular regions, respectively, and the bolometric luminosity, L_X is calculated within a virial radius r_{500} . Here r_{500} is defined as the radius within which the average matter density is equal to $\Delta_c = 500$ times the critical density of the Universe at the cluster redshift.

It is worth noting that we found no clear redshift evolution of the β -model parameters and of the temperature at $z < 0.5$ (see Ota & Mitsuda 2004 for details). We also examined the redshift dependence of the L_X-T relation by evaluating the relations for three subsets of data, 18 clusters in $0.1 \leq z < 0.2$, 27 clusters in $0.2 \leq z < 0.3$, and 24 clusters in $0.3 \leq z < 0.56$ (only 7 out of 24 have $z > 0.4$) and by comparing with the previous results. There is a marginal trend to obtain a steeper slope and a smaller normalization factor for the higher redshfit clusters.

$$L_X = 1.23_{-0.95}^{+2.62} \times 10^{43} (kT)^{2.75_{-0.71}^{+0.85}} \text{ for } 0.1 \leq z < 0.2, \quad (1)$$

$$L_X = 5.13_{-4.23}^{+19.0} \times 10^{42} (kT)^{3.18_{-0.84}^{+0.92}} \text{ for } 0.2 \leq z < 0.3, \quad (2)$$

$$L_X = 2.95_{-2.92}^{+108.5} \times 10^{41} (kT)^{4.65_{-1.86}^{+2.33}} \text{ for } 0.3 \leq z < 0.56. \quad (3)$$

Ettori et al. (2004) reported a steep slope of 3.72 ± 0.47 (1σ error) for high redshift clusters ($0.4 < z < 1.3$) based on the *Chandra* data analysis and suggested a negative evolution. Our results agree with their relation within the errors. Thus there might be a weak redshift evolution in the L_X-T relation. However, due to the large uncertainties associated with the relations for the higher redshifts, it is not statistically significant. We then carry out statistical studies regardless of their redshifts in this paper.

3 STATISTICAL ANALYSIS

3.1 $L_X - T$ Relation and Gas Density Profiles

Since the $L_X - T$ relation is sensitive to the ICM structure of the core region, we first examine the core radius. As noted in Ota & Mitsuda (2002), the r_c distribution exhibits high concentrations around 50 and 200 h_{70}^{-1} kpc (Fig. 2b). Furthermore the $L_X - T$ shows a significant offset if the sample is divided into two subgroups according to the core radius (i.e., for a fixed temperature a small-core cluster tends to be brighter than a large-core cluster; see also Fig. 1a):

$$L_X = 1.05_{-0.11}^{+0.12} \times 10^{43} (kT)^{3.01} \text{ for } r_c < 0.1 \text{ Mpc}, \quad (4)$$

$$L_X = 4.52_{-0.34}^{+0.37} \times 10^{42} (kT)^{3.01} \text{ for } r_c > 0.1 \text{ Mpc}. \quad (5)$$

Under the self-similar model, the internal structure of the gas should be scaled by the virial radius, and then r_{500}/r_c should be constant for all clusters. However, as seen from Figure 2a, r_c does not simply scale by r_{500} . If we divide the sample into two r_c groups relative to $r_c = 100$ kpc, we obtain $r_{500} \propto r_c^{0.37_{-0.11}^{+0.12}}$ for 34 clusters with $r_c > 100$ kpc while no meaningful correlation was found for 35 clusters with $r_c < 100$ kpc (the correlation coefficient is 0.21). This clear departure from the self-similar relation particularly for the small-core clusters suggests that the formation of the small cores are determined from some physical process other than the self-similar collapse.

To investigate the global gas density structure, we plot the best-fit β -model profiles for 69 clusters in Figure 3, where the radius was normalized by r_{500} . A significant scatter of the density exists within $\sim 0.1r_{500}$ region (typically $0.1r_{500} \sim 100$ kpc) and the smaller core clusters show a systematically higher density in comparison to the large core clusters. On the other hand, the profiles are fairly universal outside that radius. We consider that this is consistent with the similarity found in outer regions of scaled profiles for nearby clusters (Neumann & Arnaud 1999). In addition, by calculating the $L_X - T$ relation inside/outside a radius $0.2r_{500}$, we confirmed that the core emission is indeed a source of the scatter seen in the $L_X - T$ relation.

3.2 X-ray Fundamental Plane

Another important finding is the existence of the X-ray fundamental plane for the distant clusters (Fig. 4a). The presence of a planar distribution of nearby clusters in the 3-D parameter space (the central electron density n_{e0} , r_c , T) was first noted by Fujita & Takahara (1999). By utilizing a similar method, we obtained the following three orthogonal parameters:

$$X \propto n_{e0}^{0.44} r_c^{0.65} T^{-0.62}, \quad (6)$$

$$Y \propto n_{e0}^{0.45} r_c^{0.44} T^{0.78}, \quad (7)$$

$$Z \propto n_{e0}^{0.78} r_c^{-0.62} T^{-0.10}, \quad (8)$$

confirming the agreement with those for the nearby sample. In Figure 4b, we also show the distribution of nearby clusters projected onto the same $\log X - \log Z$ plane. We further found that by setting $X \sim$ constant, Equation (8) yields

$$Z \propto r_c^{-1.78} T^{1.00} \propto n_{e0}^{1.20} T^{-0.69}. \quad (9)$$

Thus the principal axis of the fundamental plane, Z , is suggested to be closely related to r_c . Since $t_{\text{cool}} \propto \sqrt{T}/n_{e0}$, Equation (9) can be rewritten as

$$Z \propto t_{\text{cool}}^{-1.2}. \quad (10)$$

Since the Z -axis represents a direction along which the dispersion of the data points becomes the largest in the parameter correlations, t_{cool} is considered to be a key parameter to control the ICM evolution. Hence we will focus on the effect of gas cooling in the next section.

3.3 $L_X - T$ Relation and Cooling Time

As already mentioned in the previous section, there is a large dispersion of the gas density inside $0.1r_{500}$ region which is strongly related with r_c (Fig. 3). Ota & Mitsuda (2004) derived the $n_{e0} - r_c$ relation to be

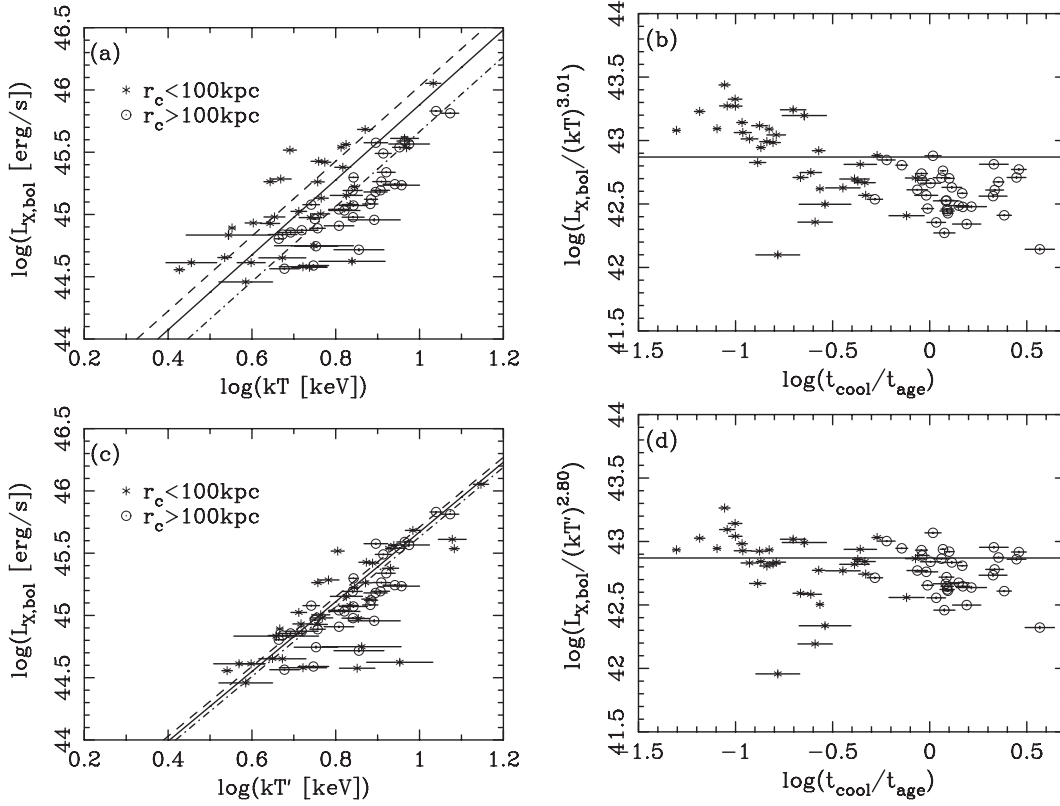


Fig. 1 L_X - T relation and t_{cool} . Upper panels, L_X - T relation of clusters (a), and $L_{1\text{keV}}$ as a function of $t_{\text{cool}}/t_{\text{age}}$ (b). Bottom panels, the luminosity to the ‘ambient temperature’ relation, $L_X - T'$ (c) and $L_{1\text{keV}} = L_X/(kT')^{2.80}$ as a function of $t_{\text{cool}}/t_{\text{age}}$ (d). In the panels (c) and (d), for clusters with short cooling timescale of $\log t_{\text{cool}}/t_{\text{age}} < -0.5$, the temperature decrease is corrected with $T' = 1.3T$, otherwise $T' = T$ (see Section 3.4).

$n_{e0} \propto r_c^{-1.3}$ and noted that the correlation tends to become even steeper for small core clusters: $n_{e0} \propto r_c^{-1.9}$ for $r_c < 100$ kpc. For clusters with such high density cores, radiative cooling may work considerably. It is also suggestive that $0.1r_{500}$ is roughly equal to the typical cooling radius of $r_{\text{cool}} \sim 100$ kpc.

In Figure 5a we show the radiative cooling time against the core radius. We confirm that for all small core clusters, it is shorter than the Hubble time ($t_H = 13.4$ Gyr; Spergel et al. 2003), $t_{\text{cool}} < t_H$. Furthermore, considering the strong dependence on the core radius, $t_{\text{cool}} \propto r_c^{1.7}$ for $r_c < 100$ kpc (Ota & Mitsuda 2004), these results seem to indicate a central concentration of the gas according to the progress of radiative cooling. This may be considered a support to the standard cooling-flow model (Fabian et al. 1994) in this regard. However, as seen from Figure 5b, there is no clear difference in temperature between the two subgroups of different core sizes. The average temperature (and the standard deviation) is 5.4 keV (1.8 keV) for the clusters with $r_c < 100$ kpc and 7.0 keV (1.8 keV) for $r_c > 100$ kpc, and the difference is only 30%. Thus there is not a strong temperature drop as predicted by the standard cooling-flow model. Our result confirms the lack of strongly cooled gas based on the large sample of *ROSAT* and *ASCA* clusters.

3.4 L_X - T' Relation and Cooling Time

To investigate the nature of the dispersion around the L_X - T relation in more detail, we introduce $L_{1\text{keV}} \equiv L_X(kT/1 \text{ keV})^{-\alpha}$ (α : the best-fit power-law index) and show $L_{1\text{keV}}$ as a function of the cooling time normalized by the age of the universe at the cluster redshift, ($t_{\text{cool}}/t_{\text{age}}$) in Figure 1b. At $\log(t_{\text{cool}}/t_{\text{age}}) >$

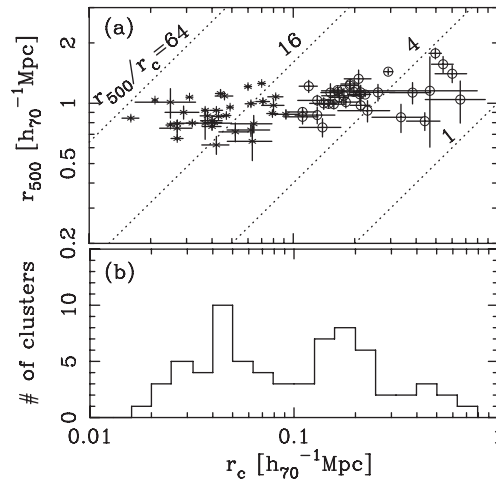


Fig. 2 (a) The r_{500} - r_c relation and (b) histogram of r_c for 69 clusters. In the panel (a), 35 clusters with small core of $r_c < 100$ kpc and 34 clusters with larger core of $r_c > 100$ kpc are shown with the asterisks and the circles, respectively. The dotted lines indicate the self-similar condition corresponding to four different constant values of r_{500}/r_c .

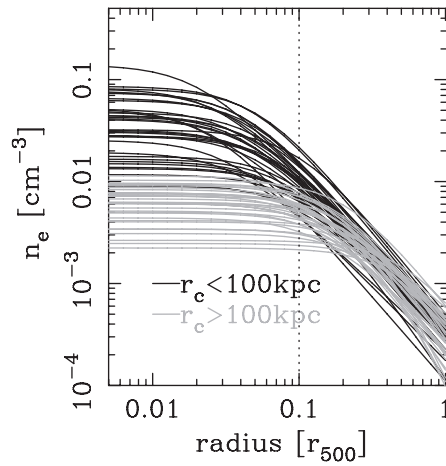


Fig. 3 Electron density profiles for 69 clusters. The best-fit density profiles derived with the single β -model are plotted, where the radius is normalized with r_{500} . $0.1r_{500}$ is indicated with the vertical dotted line, inside which the scatter is the most prominent.

-0.5 the distribution is nearly constant within the data scatter. On the other hand, at the shorter cooling time of $\log(t_{\text{cool}}/t_{\text{age}}) \ll -0.5$, a significant deviation from the mean L_X - T relation (which is denoted with the horizontal solid line in the figure) is clearly visible. Although this was interpreted as central excess emission accompanied by the radiative cooling within the framework of the standard cooling-flow model, we want to suggest the possibility that this might be due to the underestimate of the temperature for its mild decrease at the center of clusters with short cooling time.

We then evaluate the emission weighted temperature of the clusters with short cooling time utilizing the universal temperature profile found in many nearby cooling-flow clusters. Assuming a projected

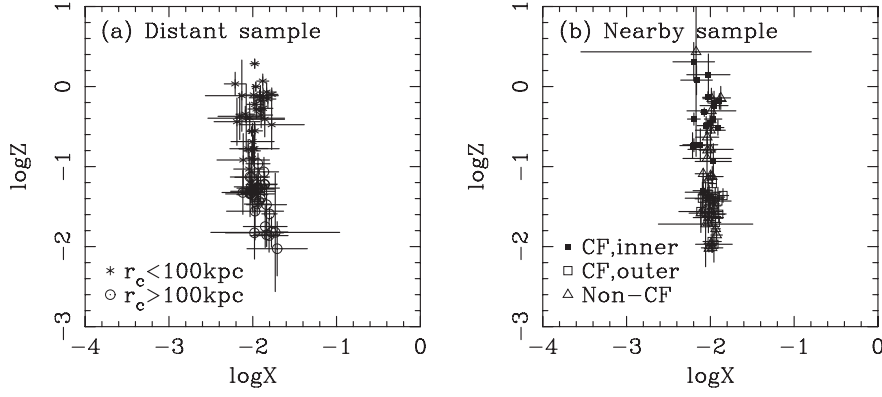


Fig. 4 Results of X-ray fundamental plane analysis. In panel (a), the best-fit $\log X - \log Z$ plane obtained for the distant clusters is shown. The meaning of the symbols are the same as Fig. 2. In the panel (b), 45 nearby clusters taken from Mohr et al. (1999) were projected onto the same fundamental plane as panel (a). According to table 2 of Mohr et al. (1999) non cooling-flow clusters are shown with the triangles, and inner-core and outer-core components of cooling-flow clusters are separately shown with the solid boxes and open boxes.

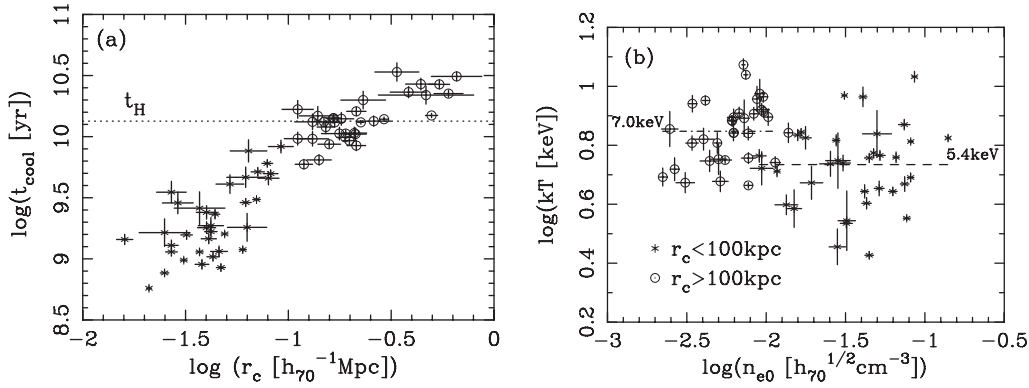


Fig. 5 $t_{\text{cool}}-r_c$ (a) and $T-n_{e0}$ (b) relations. For panel (a), t_{cool} is the radiative cooling timescale (see text). There is a strong correlation with r_c which follows $t_{\text{cool}} \propto r_c^{1.7}$. The Hubble time, $t_H = 13.4$ Gyr is indicated with the horizontal dotted line. Then $t_{\text{cool}} < t_H$ for all clusters belonging to the smaller core group. For panel (b), n_{e0} is the central electron density obtained from the β model analysis. There is no clear difference in the temperature range between the two subgroups though n_{e0} is scattered nearly over two orders of magnitudes. Their average temperatures of 5.4 keV and 7.0 keV are shown with the dashed line and dot-dash line, respectively.

temperature profile, $T(r) \propto 0.40 + 0.61[(x/x_c)^{1.9}/(1 + (x/x_c)^{1.9})]$ ($x = r/r_{2500}$) for relaxed clusters (Allen et al. 2001) and the β profile for the brightness, $S(r) \propto (1 + (r/r_c)^2)^{-3\beta+1/2}$, we obtain $T = \int_0^{r_{\text{max}}} T(r)S(r)2\pi r dr / \int_0^{r_{\text{max}}} S(r)2\pi r dr$. Since the temperature profile is nearly constant outside the typical cooling radius of ~ 100 kpc, we estimate a temperature of the outer, non-cooling region, T' to be

$$T' \sim 1.3T, \tag{11}$$

for the typical values of $r_c = 50$ kpc, $\beta = 0.6$, $r_{2500} = 600$ kpc and $r_{\text{max}} = 1$ Mpc.

By simply adopting the correction $T' = 1.3T$ for 26 clusters with $\log(t_{\text{cool}}/t_{\text{age}}) \leq -0.5$ otherwise $T' = T$ for 43 clusters, we plot the L_X-T' relation in Figure 1c. As shown below, the difference in the

normalization factors between $r < 100$ and > 100 kpc mostly disappeared in this case.

$$L_X = 8.04_{-0.65}^{+0.71} \times 10^{42} (kT')^{2.80} \text{ for } r_c < 0.1 \text{ Mpc}, \quad (12)$$

$$L_X = 6.76_{-0.35}^{+0.56} \times 10^{42} (kT')^{2.80} \text{ for } r_c > 0.1 \text{ Mpc}. \quad (13)$$

It is thus remarkable that after the correction, there is no significant difference in the dispersion of the data points between $t_{\text{cool}} < t_{\text{age}}$ and $t_{\text{cool}} > t_{\text{age}}$, and $L_{1\text{keV}}$ can be regarded as constant within the data scatter over 2 orders of magnitude of t_{cool} (Fig. 1d). The slope of the power-law function is $2.80_{-0.24}^{+0.28}$ and thus marginally less steep compared with that of $L_X - T$.

4 DISCUSSION

4.1 Comparisons with Nearby Clusters

Based on the systematic analysis of the distant sample, we have shown that there is a significant offset in the L_X - T relation between the small-core and large-core clusters as well as the scatter is tightly connected with the radiative cooling time in the core region. We compare below our results with the scaling relation of nearby clusters. Recently O'hara et al. (2006) and Chen et al. (2007) classified their nearby samples into Cool Core (CC) clusters and non Cool Core (NCC) clusters and showed a segregation of the two groups on the $L_X - T$ plane, which is basically consistent with our results. Note that they used slightly different definitions. However, the CC cluster is in general one having a cooling core at the center and the cooling time shorter than the Hubble time. O'hara et al. (2006) further attempted to explain the observed data points by using the L_X - $T - I_0$ relation (I_0 is the central X-ray surface brightness) and found the temperature scaling of ($T_X/1.38$) which would minimize the scatter around the mean scaling relation. This is in a good agreement with our present results. They also noted that the CC clusters, which usually have less morphological substructure, exhibit higher intrinsic scatter about scaling relation even after correcting for the cooling core effect, suggesting that a more global process is at work. Thus the residual variation of $L_{1\text{keV}}$ for the small r_c clusters in the present study may be related to the scatter found by O'hara et al. (2006) though we did not find a significant difference of the $L_{1\text{keV}}$ distribution between the small-core/large-core clusters. On the other hand, Vikhlinin et al. (2006) reported based on the *Chandra* observations that the incidence rate of the cooling core phenomenon is smaller at high redshift ($z > 0.5$). Therefore these multiple observational studies indicate that we might be looking at the progress of radiative cooling in the core region. However, the previous analyses were based on the different analysis methods and thus a uniform analysis of clusters in a wide redshift range is considered to be important to further clarify the redshift evolution of the core structure.

4.2 Possibility of Quasi-Hydrostatic State of the ICM

The observational results indicate that the gas in the core region of small core clusters is undergoing radiative cooling but the temperature decline towards the center seems mild. The gas may be considered close to a steady state. We will discuss such a possible state of the gas, quasi-hydrostatic cooling, proposed by Masai & Kitayama (2004). The model predicts a moderate and smooth gas inflow with hydrostatic balancing. In the context, unlike isobaric cooling flows that increase the local density so the thermal pressure $P(r)$ is kept against local cooling, quasi-hydrostatic cooling allows the gas to modify its profile or core size so $\nabla P(r)$ matches with the force by gravitational potential.

In Section 3.4 we derived the L_X - T' relation by correcting the emission-weighted temperature for small-core clusters with short t_{cool} based on the idea of the universal temperature profile, and showed that the bolometric luminosity normalized by the temperature dependence of $(kT')^{2.8}$, $L_{1\text{keV}}$ is constant within the data scatter over a wide range of $t_{\text{cool}}/t_{\text{age}}$. This strongly suggests that the rate of thermal energy loss is kept nearly constant after the onset of cooling in the cluster core.

According to the quasi-hydrostatic model, the temperature starts to decrease at the cooling radius and approaches a constant of $\sim 1/3$ the ambient temperature towards the center. The temperature profile does not depend on its absolute value. This picture may explain the observations of nearby cooling-flow clusters. The mass inflow rate from the outer region is controlled by cooling so to maintain the quasi-hydrostatic balance and it is expected to vary little through the flow. The condition is well satisfied in the case that the temperature is $kT \gtrsim 2$ keV where bremsstrahlung dominates cooling more than line emission. The present

sample meets this condition since it has a temperature range of $2 < kT$ [keV] < 12 . Therefore our results can be consistently understood within a framework of the quasi-hydrostatic cooling model.

As described above, cooling with quasi-hydrostatic balancing modifies the core structure of the gas. This may give a clue to the origin of the small core of ~ 50 kpc or the inner core component of the double- β cluster. In addition the study would also have an impact on the present understanding of the origin of the dispersions around the L_X-T relation because it provides the observational evidence that they are directly linked to the thermal evolution of the ICM. Besides, this study shows how the relation would be modified when the effect of the cooling is considered.

4.3 Morphological Evolution of X-ray Clusters

Finally we comment on a phenomenological view on the morphological evolution of the ICM. According to the X-ray morphology examined in Section 2, we can divide the sample into three subgroups: the regular single- β cluster, the irregular single- β cluster, and the regular double- β cluster. To see if how they are distributed in the parameter space, we show in Figure 6 the $L_X-T'\beta$ relation and the $L_{1\text{keV}} - (t_{\text{cool}}/t_{\text{age}})$ diagram. Note that $T'\beta$ was used instead of T' since under the virial theorem and the β -model the virial temperature is given by $T_{\text{gas}}\beta$ rather than T_{gas} (Akahori & Masai 2005; Ota et al. 2006) and it is worth examining. We can see in Figure 6b a trend of morphological change along the horizontal axis (\sim the principal axis Z ; see Section 3.2). According to the level of cooling and different density structures, it is possible to define three phases of the ICM evolution as follows: from larger to smaller t_{cool} , i) the irregular large-core clusters at $\log(t_{\text{cool}}/t_{\text{age}}) \gtrsim 0$, where a large scatter of $L_{1\text{keV}}$ is seen, ii) the regular large-core clusters at $-0.3 \lesssim \log(t_{\text{cool}}/t_{\text{age}}) < 0$, and iii) the regular small-core clusters at $\log(t_{\text{cool}}/t_{\text{age}}) < -0.3$. Furthermore, the double- β clusters are located in iii) $\log(t_{\text{cool}}/t_{\text{age}}) \lesssim -0.3$, the same region as the regular small-core clusters. As the inner-/outer-core dominant double- β clusters are at a shorter/longer side of the range, they are suggested to be closely related to the small-/large-core regular clusters. We thus consider that this may be connected with the evolution of the X-ray surface brightness distribution after the onset of radiative cooling. It is likely that the double- β clusters are those in the transient phase of their cooling cores, i.e., core size transition from outer-core dominated to inner-core dominated, mentioned in the quasi-hydrostatic cooling model. As the interpretation of the double core nature, we consider in the following

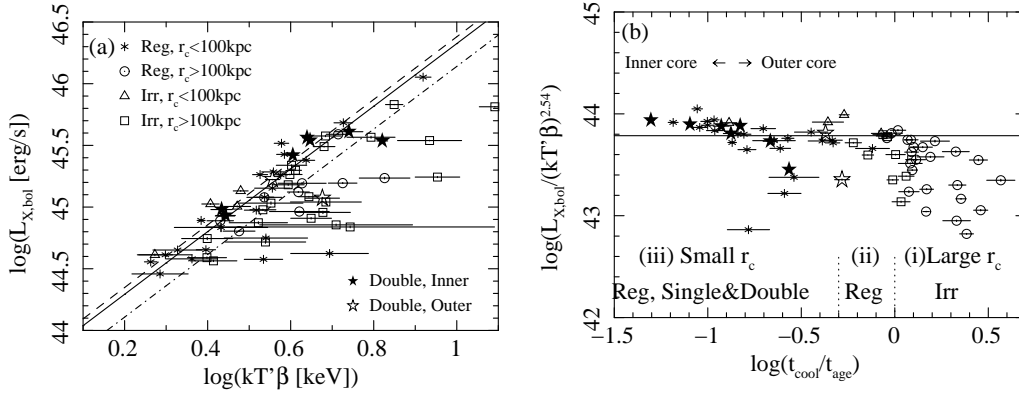


Fig. 6 $L_X-T'\beta$ relation and X-ray morphology. The regular single- β clusters with r_c smaller (larger) than 100 kpc are shown with the asterisk (circles), and the irregular single- β clusters with smaller (larger) than 100 kpc are shown with the triangles (boxes). The double- β clusters are denoted with the light-blue stars. The filled (open) stars correspond to the inner-core (outer-core) dominant double- β clusters. In the panel (b), we indicated the three phases according to the different level of cooling and density structure: i) the large core, irregular clusters with long t_{cool} relative to t_{age} , ii) the large core, regular clusters with moderate t_{cool} , and iii) the small core, regular clusters with short t_{cool} . In the phase iii), 9 of the sample shows the significant double- β structure, and the inner-core/outer-core dominant double- β clusters are located at the shorter/longer cooling time (see Sect. 4.3).

way: when some time passed after the collapse and the cooling becomes important, the core is radiatively cooled and the central density gradually becomes higher to evolve from an outer-core-dominant cluster toward an inner-core-dominant cluster. See Ota et al. (2006) for more details.

5 SUMMARY

From the statistical analysis of 69 clusters in $0.1 < z < 0.56$ with the *ROSAT* and *ASCA* X-ray catalog, we have obtained the following main results.

1. Regarding the cluster outer region, the density profiles are found to be nearly universal. On the other hand, for the central region, the gas density exhibits a significant scatter and the self-similar condition is not satisfied, particularly in the small-core clusters.
2. We investigated the redshift evolution of the L_X - T relation. There might be a weak, negative evolution, however, it is not significant within the present statistics.
3. We investigated the parameter correlations focusing on the L_X - T relation and the connection to r_c and t_{cool} , and suggested based on the X-ray fundamental plane analysis that t_{cool} is likely to be a control parameter for the ICM structure of the cluster core region.
4. The observational results indicate that the gas in the central region of small-core clusters is undergoing radiative cooling, but the temperature decrease is mild: once the temperature bias is corrected using $T' = 1.3T$, $L_{1\text{keV}}$ can be regarded as constant against t_{cool} . This strongly suggests that some steady state is realized in the small-core clusters. The present results can be consistently understood within the framework of the quasi-hydrostatic model.
5. From the L_X - $T'\beta$ relation, we showed that $L_{1\text{keV}}$ is related to the X-ray morphology. We indicated the three possible phases of the gas property along the t_{cool} axis and draw a phenomenological picture of the ICM evolution.

We have also shown that there is a significant offset between the small core/large core clusters on the $L_X - T$ plane, which is consistent with the CC/NCC segregation reported for the nearby cluster samples. To further clarify the redshift evolution of the core structure, we consider that it is necessary to perform a uniform analysis covering a wide redshift range.

References

- Allen S. W., Schmidt R. W., Fabian A. C., 2001, *MNRAS*, 328, L37
 Akahori, T., Masai K., 2005, *PASJ*, 57, 419
 Cavaliere A., Fusco-Femiano R., 1976, *A&A*, 49, 137
 Cavaliere A., Menci N., Tozzi P., 1997, *ApJ*, 484, L21
 Chen, Y., Reiprich, T. H., Böhringer H., Ikebe Y., Zhang Y.-Y., 2007, *A&A*, 466, 805
 David L. P. et al., 1993, *ApJ*, 412, 479
 Edge A. C., Stewart G. C., Fabian A. C., Arnaud K. A., 1990, *MNRAS*, 245, 559
 Ettori S., Tozzi P., Borgani S., Rosati P., 2004, *A&A*, 417, 13
 Evrard A. E., Henry J. P., 1991, *ApJ*, 383, 95
 Fabian A. C., Crawford C. S., Edge A. C., Mushotzky R. F., 1994, *MNRAS*, 267, 779
 Fujita Y., Takahara F., 1999, *ApJ*, 519, L51
 Kaastra J. S. et al., 2004, *A&A*, 413, 415
 Kaiser N., 1986, *MNRAS*, 222, 323
 Masai K., Kitayama T., 2004, *A&A*, 421, 815
 Mohr J. J., Mathiesen B., Evrard A. E., 1999, *ApJ*, 517, 627
 Neumann D. M., Arnaud M., 1999, *A&A*, 348, 711
 Neumann D. M., Arnaud M., 2001, *A&A*, 373, L33
 O'Hara T. B., Mohr J. J., Bialek J. J., Evrard A. E., 2006, *ApJ*, 639, 64
 Ota N., Mitsuda K., 2002, *ApJ*, 567, L23
 Ota N., Mitsuda K., 2004, *A&A*, 428, 757
 Ota N., Kitayama T., Masai K., Mitsuda K., 2006, *ApJ*, 640, 673
 Spergel D. N. et al., 2003, *ApJS*, 148, 175
 Vikhlinin A. et al., 2006, arXiv:astro-ph/0611438
 Voit G. M., 2005, *Reviews of Modern Physics*, 77, 207